



Lawrence Berkeley Laboratory

UNIVERSITY OF CALIFORNIA

EARTH SCIENCES DIVISION

To be presented at the 1991 ASME/AIChE National Heat Transfer Conference Session on Engineering Models in Multiphase Flow, Minneapolis, MN, July 28-31, 1991, and to be published in the Proceedings

A Mathematical Model for Two-Phase Water, Air, and Heat Flow Around a Linear Heat Source Emplaced in a Permeable Medium

C. Doughty and K. Pruess

March 1991



1 LOAN COPY
1 Circulates
1 for 4 weeks

Bldg. 50 Library.

Copy 2

LBL-30050

DISCLAIMER

This document was prepared as an account of work sponsored by the United States Government. While this document is believed to contain correct information, neither the United States Government nor any agency thereof, nor the Regents of the University of California, nor any of their employees, makes any warranty, express or implied, or assumes any legal responsibility for the accuracy, completeness, or usefulness of any information, apparatus, product, or process disclosed, or represents that its use would not infringe privately owned rights. Reference herein to any specific commercial product, process, or service by its trade name, trademark, manufacturer, or otherwise, does not necessarily constitute or imply its endorsement, recommendation, or favoring by the United States Government or any agency thereof, or the Regents of the University of California. The views and opinions of authors expressed herein do not necessarily state or reflect those of the United States Government or any agency thereof or the Regents of the University of California.

**A Mathematical Model for Two-Phase Water, Air, and Heat Flow
around a Linear Heat Source Emplaced in a Permeable Medium**

Christine Doughty and Karsten Pruess

Earth Sciences Division
Lawrence Berkeley Laboratory
University of California
Berkeley, California 94720

March 1991

This work was supported by the Yucca Mountain Project, Sandia National Laboratories, under Document No. SNL 54-1064, and by the Director, Office of Energy Research, Office of Basic Energy Sciences, Engineering and Geosciences Division, of the U.S. Department of Energy under Contract No. DE-AC03-76SF00098.

ABSTRACT

A semianalytical solution for transient two-phase water, air, and heat flow in a uniform porous medium surrounding a constant-strength linear heat source has been developed, using a similarity variable $\eta = r/\sqrt{t}$ (r is radial distance, t is time). Although the similarity transformation requires a simplified radial geometry, all the physical mechanisms involved in two-phase fluid and heat flow may be taken into account in a rigorous way. The solution includes nonlinear thermophysical fluid and material properties, such as relative permeability and capillary pressure variations with saturation, and density and viscosity variations with temperature and pressure. The resulting governing equations form a set of coupled nonlinear ODEs, necessitating numerical integration. The solution has been applied to a partially saturated porous medium initially at a temperature well below the saturation temperature, which is the setting for the potential nuclear waste repository site at Yucca Mountain, Nevada. The resulting heat and fluid flows provide a stringent test of many of the capabilities of numerical simulation models, making the similarity solution a useful tool for model verification. Comparisons to date have shown excellent agreement between the TOUGH2 simulator and the similarity solution for a variety of conditions.

A semianalytical solution has been developed for transient two-phase water, air, and heat flow in a porous medium surrounding a constant-strength linear heat source, using a similarity variable $\eta = r/\sqrt{t}$. While the similarity transformation approach requires a simplified radial geometry, all the complex physical mechanisms involved in coupled two-phase fluid and heat flow can be taken into account in a rigorous way, so the solution may be applied to a variety of problems of current interest.

Application of the similarity solution approach to two-phase fluid and heat flow problems in radial geometry was pioneered in the geothermal well test studies of Grant [1] and O'Sullivan [2]. Grant developed a quasi-analytic approach for the analysis of geothermal wells producing from two-phase reservoirs, using an approximate linearization of the governing equations. O'Sullivan recognized that the similarity variable concept can be used to obtain solutions that include all nonlinearities of the governing equations in a rigorous way.

Our work was motivated by a desire to predict the thermohydrological response to the potential geologic repository for heat-generating high-level nuclear wastes at Yucca Mountain, Nevada, in a partially-saturated, highly-fractured volcanic

formation. The geometric simplifications required by the similarity solution preclude detailed predictions of the behavior of the repository as a whole, but the solution can be used to gain insight into the impact of various flow and heat transport parameters on physical conditions near the waste canisters. Other problems that can be studied involve heat sources such as buried power-transmission cables, volcanic dikes, agricultural root-zone heating operations, and underground thermal energy storage systems. Furthermore, the ability to rigorously solve a class of highly nonlinear two-phase fluid and heat flow problems has important applications in the verification of complex numerical simulators.

THERMAL AND HYDROLOGIC CONDITIONS NEAR THE HEAT SOURCE

The ambient conditions in the partially saturated formation around the potential nuclear waste repository at Yucca Mountain, Nevada ($P_0 = 0.89$ bars, $T_0 = 20^\circ\text{C}$, $S_{l0} = 0.8$) are such that T is well below the saturation temperature ($T_{\text{sat}} = 96^\circ\text{C}$), so water is primarily in the liquid phase, and the initial heat transfer in the host rock is mainly conductive. As the temperature around a waste package (the heat source) increases to the saturation temperature, evaporation increases and vapor partial pressure

becomes appreciable. A convective heat-transfer mechanism known as a heat pipe may contribute to or even dominate heat transfer in this regime. Near the heat source, liquid water vaporizes, causing pressurization and an out-flow of the gas phase, which is composed of noncondensable air and water vapor. The water vapor condenses in cooler more distant regions, depositing its latent heat of vaporization. This creates a nonuniform saturation profile, with liquid saturation increasing with distance from the heat source. The saturation gradient drives the counter-flow of the liquid phase toward the heat source through capillary forces. The liquid then vaporizes again and repeats the cycle. With time the heat pipe moves away from the waste canister, leaving a gas-phase zone in which heat transfer is again conduction-dominated. The conditions surrounding a waste package at some time after emplacement are shown schematically in Figure 1.

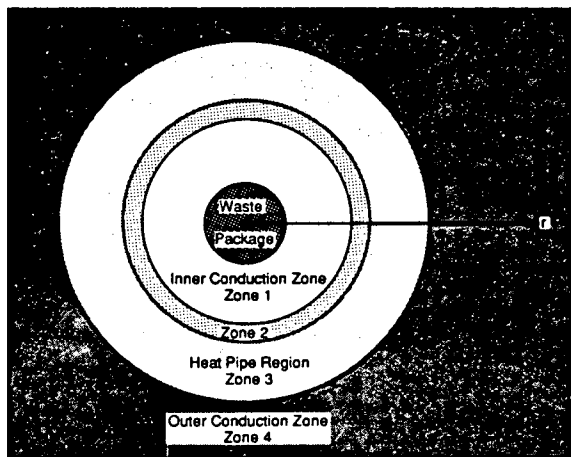


Figure 1. Schematic of the conditions achieved at some time after waste emplacement (not to scale). Water is primarily in the liquid phase in zone 4, because $T < T_{sat}$; two-phase conditions prevail in zones 2 and 3, with $T = T_{sat}$; fluid in zone 1 is in the gas phase, with $T > T_{sat}$.

The convective heat transfer of the heat-pipe region is accompanied by small temperature gradients, whereas in the conductive regions temperature gradients are large. Thus, conditions at the waste package may vary greatly depending on the relative importance of conductive and

convective heat transfer. If an extensive heat pipe develops, the temperature will remain near the saturation temperature (about 100°C) for long times. Under these conditions, air will be purged from the near-canister region, leaving a gas phase composed purely of water vapor (steam). If heat transfer is primarily conductive, a gas-phase zone, or two-phase zone with only a small amount of immobile liquid, will develop around the waste package. Temperatures may be very high and air is more likely to be present.

The basic requirements for heat-pipe development are (1) the presence of a volatile fluid and (2) a mechanism by which gas-phase fluid can flow away from the heat source and liquid-phase fluid toward it. The groundwater surrounding a geologic nuclear waste repository will be volatile only if the heat-generating capacity of the wastes, coupled with the low thermal conductivity of rock, raises the temperature near the canisters above the saturation temperature of water (T_{sat}) under prevailing pressure conditions. For gas-phase flow away from the heat source to occur, the far-field pressure must be lower than the pressure at the heat source. Liquid-phase flow requires a driving force toward the heat source, which could be gravity, capillary pressure, or a combination of both. Finally, there must be sufficient permeability to both phases to establish the counter-flow necessary for a heat pipe.

For a partially saturated repository environment ambient pressure is near 1 bar and $T_{sat} \approx 100^\circ\text{C}$. In contrast, for a deep water-saturated formation fluid pressure at the waste packages (backfill pressure) is likely to be much greater than 1 bar, with the far-field pressure even larger. This makes heat-pipe development unlikely because a) temperatures may never increase as high as T_{sat} ; and b) there is no driving force for gas-phase flow away from the heat source when backfill pressure is less than far-field pressure.

METHODOLOGY

The governing equations for two-phase fluid and heat flow for water and air in a porous medium are summarized by Doughty and Pruess [3], and the basic processes represented by the equations are outlined

below. A conservation law balances accumulation M and flux Q of each component (water, air, energy), assuming local thermodynamic equilibrium between water, air, and rock. The fluid flux terms include Darcy's law modified for two-phase flow using relative permeability and capillary pressure functions, and binary diffusion between water vapor and air in the gas phase. The inclusion of capillary pressure (which we define as $P_c = P_l - P_g$, making P_c a negative quantity) allows the possibility of liquid and gas phase counter-flow. Gas-phase pressure is the sum of air and vapor partial pressures, $P_g = P_a + P_v$. Both the relative permeability and capillary pressure functions are highly nonlinear functions of liquid saturation. The heat balance includes conductive and convective terms with phase-change effects and transport of latent heat. Realistic equations of state for water [4] and air (ideal gas with Henry's law for dissolution in the liquid phase) are used. With these assumptions, the conservation laws form a set of three coupled nonlinear second-order partial differential equations, which are mathematically equivalent to a set of six nonlinear coupled first-order partial differential equations. For single-phase conditions, the six primary dependent variables (unknowns) are temperature T , pressure P , air partial pressure P_a , water flux Q_w , air flux Q_a , and heat flux Q_e . Under two-phase conditions, gas saturation S_g replaces temperature as a primary variable, as temperature can be determined directly from other primary variables through the saturation curve and a vapor pressure lowering correction.

To achieve the symmetry required for the similarity solution approach, the geologic medium is assumed to be uniform and isotropic, the heat source is modeled as an infinitely long cylinder, and gravity is neglected. The geometry of the problem then reduces to radial symmetry, with just two independent variables, radial distance r and time t . If the medium is of infinite extent with uniform initial conditions, and boundary conditions are applied only at $r = 0$ (a line source) and $r = \infty$, and are time-independent, the coupled partial differential equations can be transformed into simpler ordinary differential equations (ODEs) through the use of a similarity variable, $\eta = r/\sqrt{t}$. For example, the conservation equations are

$$\frac{\partial M_m}{\partial t} + \frac{1}{2\pi r} \frac{\partial Q_m}{\partial r} = 0 \quad (1)$$

where $m = w$ (water), a (air), or e (energy), M is mass or energy per unit volume, and Q is mass or energy flow per unit thickness. After similarity transformation, this becomes

$$\frac{\eta}{2} \frac{dM_m}{d\eta} + \frac{1}{2\pi\eta} \frac{dQ_m}{d\eta} = 0. \quad (2)$$

Darcy's Law for liquid flow is

$$Q_l = -2\pi r K_l \frac{\partial P_l}{\partial r} \quad (3)$$

which becomes

$$Q_l = -2\pi\eta K_l \frac{dP_l}{d\eta}. \quad (4)$$

Other terms in the flux equations can be similarly transformed. This transformation is known as the Boltzmann transformation in the context of heat-conduction problems, and has been applied by Grant [1] and O'Sullivan [2] to geothermal well test problems.

The resulting ODEs are coupled and nonlinear, so a numerical integration from $\eta=0$ to $\eta=\infty$ is required to solve them. It proves to be convenient to use $z = \ln(\eta)$ as the integration variable. For the linear heat source representing a backfilled or 'closed-hole' nuclear waste canister, the boundary conditions are

$$z = \ln(\eta) = \ln(r/\sqrt{t}) = -\infty \quad (5)$$

$$(r = 0 \text{ or } t = \infty)$$

$$Q_w = 0 \quad Q_a = 0 \quad Q_e = Q_{e0}$$

$$P, P_a, T \text{ unknown}$$

and

$$z = \ln(\eta) = \ln(r/\sqrt{t}) = +\infty \quad (6)$$

$$(r = \infty \text{ or } t = 0)$$

$$P_g = P_0 \quad P_a = P_{a0} \quad S_g = S_{g0}$$

$$Q_w, Q_a, Q_e \text{ unknown.}$$

These boundary conditions constitute a two-point boundary value problem, in which three of the boundary conditions are specified at the $z = -\infty$ limit of integration and three are specified at the $z = +\infty$ limit. The ODEs in z set up a functional dependence between the upper and lower boundary conditions, requiring an iterative process for solution. We use an iterative integration scheme, known as the shooting method [5], which consists of a Newton-Raphson iteration on

the unknown boundary conditions $(P, P_a, T) |_{z \rightarrow \infty}$. For the numerical integration, the limits $z = \infty$ are replaced by finite values z_L and z_U (see below). At the lower limit of the integration, values are guessed for the missing boundary conditions, and the numerical integration of the coupled ODEs is carried out. At the upper limit of the integration, the values of the variables are compared to the specified boundary conditions, and refined estimates of the lower limit boundary conditions are made. This procedure, illustrated in Figure 2, continues until the value of each variable at $z = z_U$ matches the specified boundary conditions P_0, P_{a0} , and S_{g0} . A more detailed discussion of the governing equations and the similarity solution methodology is given in Doughty and Pruess [3,6].

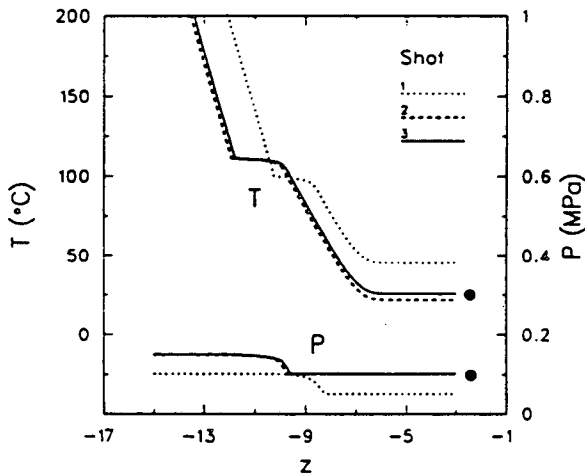


Figure 2. Temperature and pressure profiles illustrating the shooting method for a problem without air. The black dots show the temperature and pressure boundary conditions imposed at z_U .

ILLUSTRATIVE RESULTS

Figure 3 shows an example of the results of the similarity solution. Most of the parameters used to specify this problem, given in Table 1, are typical of conditions expected at the potential nuclear waste repository at Yucca Mountain, Nevada [7]. However, fracture effects are not included and the intrinsic permeability k of the rock matrix is extremely low, so in order to get a stronger heat pipe, intrinsic permeabil-

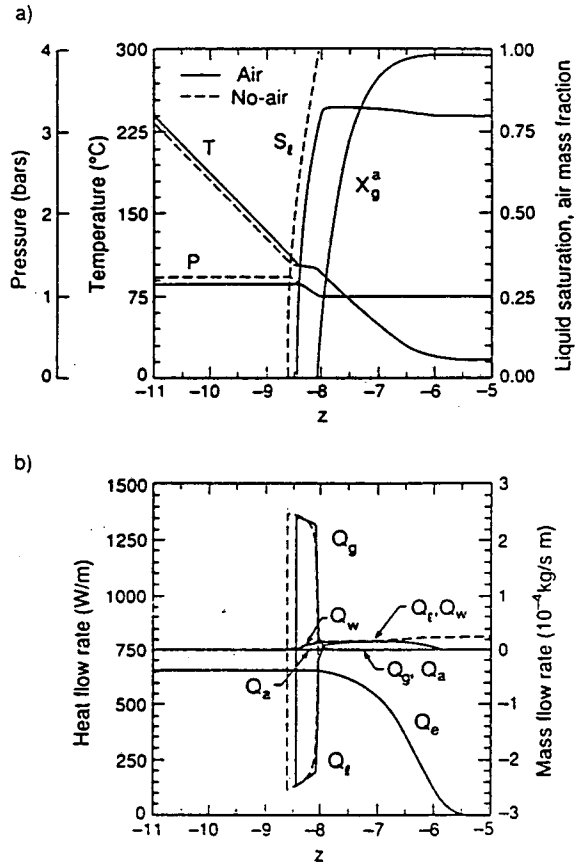


Figure 3. Results of the similarity solution for the with-air and no-air problems described in Table 1. For convenience, air mass fraction X_g^a is plotted instead of P_a .

ity has been arbitrarily increased by a factor of order 10,000, to $20 \times 10^{-15} \text{ m}^2$, and for consistency capillary pressure strength P_{c0} has been reduced by a factor $\sqrt{10,000} = 100$ in comparison to typical Yucca Mountain data. According to the definition of the similarity variable, $z = \ln(r/\sqrt{t})$, Figure 3 represents both a spatial distribution at a given time, with distance from the heat source increasing from left to right, and a time sequence at a given point in space, with time increasing from right to left; most of the discussion of figures that follow is done in terms of a spatial distribution. Figure 3 also shows the results of the similarity solution when no air is present, with other parameters unchanged from Table 1.

Table 1. Parameters for problems illustrated in Figures 3, 4, and 5. Parameters are modified from typical Yucca Mountain values, see text.

| Boundary and Initial Conditions | |
|---|---|
| $z = \ln(\eta) = \ln(r/\sqrt{t}) = -\infty$ | $Q_{o0} = 667 \text{ W/m}^*$ $Q_{w0} = 0$ $Q_{a0} = 0 \dagger$ |
| $z = \ln(\eta) = \ln(r/\sqrt{t}) = +\infty$ | $P_0 = 1 \text{ bar}$ $T_0 = 18^\circ\text{C}$ $S_{g0} = 0.2 \dagger$ |

| Material Properties | |
|--------------------------------------|--|
| $k = 20 \times 10^{-15} \text{ m}^2$ | $\kappa = 2 \text{ W/m K}$ |
| $\phi = 0.10$ | $\tau = 0.5$ |
| $\rho_s = 2550 \text{ kg/m}^3$ | $D_{va}^0 = 2.6 \times 10^{-5} \text{ m}^2/\text{s}$ |
| $c_s = 800 \text{ J/kg K}$ | |

| Characteristic Curves‡ | |
|---|-------------------------------|
| $k_{zf}(S_f) = \sqrt{S^*} \left[1 - (1 - (S^*)^{1/\lambda})^\lambda \right]^2$ | |
| $k_{rg}(S_f) = 1 - k_{zf}$ | |
| $P_c(S_f) = -P_{c0} \left[(S^*)^{-1/\lambda} - 1 \right]^{1-\lambda}$ | |
| $S^* = (S_f - S_{fr}) / (1 - S_{fr})$ | |
| $S_{fr} = 9.6 \times 10^{-4}$ | $P_{c0} = 0.125 \text{ bars}$ |
| $\lambda = 0.45$ | $P_{max} = 5000 \text{ bars}$ |

*This thermal power corresponds to high-level nuclear wastes approximately 10 years old.

†In Figure 3, used for with-air problem only.

‡Functional forms of van Genuchten [12]; P_c has been modified slightly so that as $S^* \rightarrow 0$, $P_c(S_f) \rightarrow -P_{max}$ instead of approaching $-\infty$ [3].

Overall the "with-air" and "no-air" problems show quite similar results. Of course, for the no-air problem, single-phase liquid conditions exist far from the heat source ($S_f = 1$ for $z > -8$), whereas the with-air problem is two-phase ($S_f = 0.8$), but the pressure and temperature profiles are not very different. The constant pressure and steep linear temperature profiles shown in Figure 3a for $-11 < z < -8.5$ and $-8 < z < -6.5$ indicate conductive regimes, and Figure 3b verifies that mass flow rates are small there. The more gradual temperature decline for

$-8.5 < z < -8$ coupled with a large liquid-vapor counter-flow identifies the heat-pipe region. In Figure 3b, Q_g and Q_l are the sum of the air and water components for the gas and liquid phases, respectively. Throughout this paper, the scale on which the mass flows are shown makes air flow vanishingly small, so the mass flow for each phase is essentially water flow (e.g., $Q_g = Q_w$). Note that air mass fraction X_g^a is essentially zero for $z < -8$, so the gas phase there is composed primarily of water vapor (at $z_L = -11$, $X_g^a = 10^{-24}$). The air is purged from the region near the heat source by the vapor flow away from the heat source, as would be any noncondensable gas present in the system. This could have important ramifications for waste-package design with regard to the prevention of corrosion. Extending from the cool end of the heat pipe to the heat-flow front ($-8.2 < z < -6$), there is a small liquid flow away from the heat source, indicating that not all the vapor condensing at the cool end of the heat pipe flows back toward the heat source. The out-flow is necessary because the water vapor forming at the hot end of the heat pipe is much less dense than the liquid water it replaces; it causes the heat pipe to gradually move away from the heat source.

Generally, the presence of air shortens the heat pipe from the cool end ($z = -8$ in Figure 3), by hampering the liquid-vapor counter-flow there. When air is present at the cool end of the heat pipe, liquid flow is decreased there because liquid relative permeability is lower due to the smaller liquid saturation. Vapor flow is decreased because for a given pressure gradient and gas-phase saturation only some of the mass flow is vapor, the rest being air. The heat-pipe shortening with the presence of air is evident from Figure 3, but it occurs at the hot end of the heat pipe ($z = -8.5$ in Figure 3). Because both the with-air and no-air solutions are constrained to match the same pressure and temperature boundary conditions at z_U , any difference in heat-pipe length is shifted toward z_L .

The physical processes associated with the addition of air can be demonstrated more clearly by doing a series of integrations using the no-air boundary conditions for $T(z_L)$ and $P(z_L)$, and sequentially increasing $P_s(z_L)$ from 0 to

10^{-41} to 10^{-26} bars (Figure 4). The boundary conditions at z_0 are not matched, but the effect of adding air to shorten the heat pipe is illustrated. Figure 4 shows that as the amount of air present in the system increases, X_g^a increases from zero to one at smaller values of z ; because counter-flow occurs only in regions where X_g^a is small, the heat pipe becomes shorter, leading to a greater overall temperature drop; total pressure $P = P_s + P_v$ increases; and S_l decreases because more of the pore space is filled with air. Although the values of $P_s(z_L)$ used in Figure 4 are much too small to be readily distinguished experimentally, with sufficient numerical accuracy they can be used successfully in the similarity solution. This example demonstrates one of the attractive features of the similarity solution: its usual method of employment - taking initial guesses for missing boundary conditions from results of a similar problem - provides insight into the physical effects of various problem parameters.

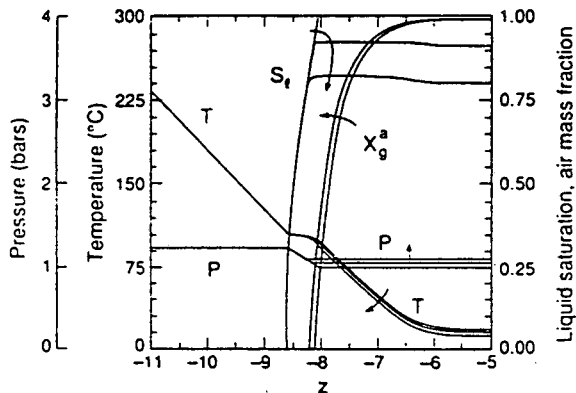


Figure 4. The effect of increasing the amount of air at z_L on the no-air problem shown in Figure 3 and described in Table 1. The arrows show the direction of change as $P_s(z_L)$ is increased from 0 to 10^{-41} to 10^{-26} bars. For comparison, for the with-air problem of Figure 3, $P_s(z_L) = 10^{-24}$ bars.

Two other differences that arise from the presence of air are also illustrated in Figure 3. The pressure decrease that occurs over the length of the heat pipe is larger for the no-air problem because, although the pressure gradient is unchanged, the heat pipe is longer. The pure liquid zone that develops for the

no-air problem for $z > -8$ has a much lower compressibility than does the low temperature two-phase zone of the with-air problem, hence the small liquid outflow extends much further from the heat source.

COMPARISON WITH THE NUMERICAL SIMULATOR TOUGH2

Multiphase fluid and heat flow problems that lack some of the symmetries required for application of the similarity variable approach must be solved by numerical simulation, using discretization of the continuous space and time variables. The accuracy and credibility of numerical simulations is a matter of serious concern, because they are subject to space and time discretization errors which are often difficult to quantify. Furthermore, numerical simulations are performed with complex computer programs, and no method is known to directly establish that such programs are free of errors. It is necessary, therefore, to test numerical simulations against known solutions that entail as many complex features as possible. The similarity solution is an ideal tool for such testing, because it gives, within the approximations of the underlying mathematical model, an essentially rigorous solution to a problem that involves the full nonlinear process complexity of transient two-phase fluid and heat flow. The idealizations made pertain only to the flow geometry and to initial and boundary conditions.

We have used the similarity solution to test the numerical simulator TOUGH2 [8,9], which calculates the flow of air and water in gaseous and liquid phases together with heat flow, using the same governing equations and equation of state as does the similarity solution. TOUGH2 employs the integral-finite-difference method to discretize space for one-, two-, or three-dimensional problems that may involve heterogeneous, anisotropic, or fractured/porous media [10]. Figure 5 shows results of TOUGH2 compared with those of the similarity solution for the problem specified in Table 1; the agreement is excellent. A one-dimensional radial mesh with 108 elements was used for the TOUGH2 calculation. The mesh spacing is nonuniform, with finest spacing (0.03 m) used where the similarity solution predicts sharp gradients. A

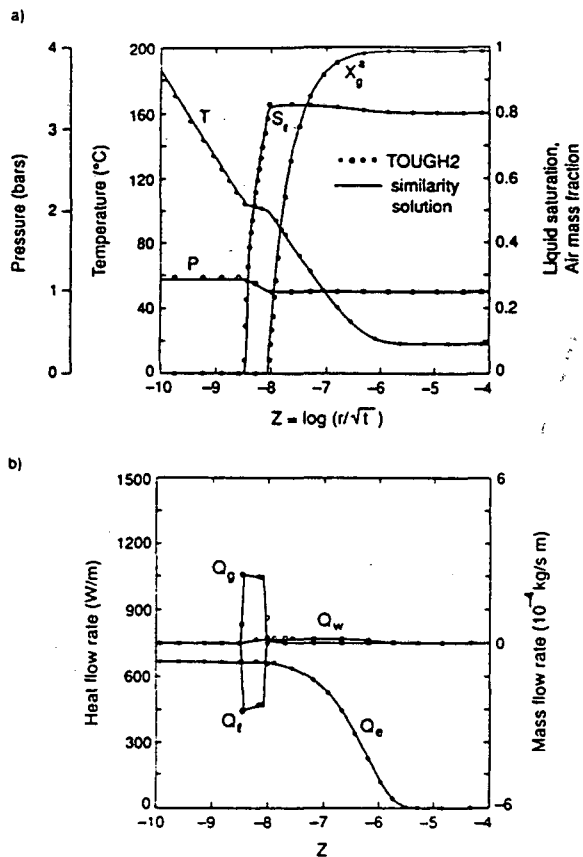


Figure 5. A comparison between results of the similarity solution and the numerical model TOUGH2 for the with-air problem described in Table 1.

heat source is placed in the innermost element ($0 < r < 0.3$ m), and the outermost element ($r = 10,000$ m) is at sufficiently large distance to remain at constant temperature, pressure, and saturation for a simulation time of 6.3 years. The TOUGH2 calculation required 800 time steps and 8.5 minutes of CPU time on the Cray X-MP at the National Energy Research Supercomputer Center at Lawrence Livermore National Laboratory.

In contrast, one numerical integration of the similarity solution (using previously-determined correct starting values at z_L) required 228 integration steps and took 2.6 CPU seconds. The shooting procedure requires four integrations per shot, and with reasonable initial guesses, usually converges within

three to five shots. The key to successful use of the similarity solution is finding reasonable initial guesses. This may require some preliminary trial integrations, the solution to a similar problem, physical intuition, or a combination of the three. Assuming five trial integrations to arrive at workable initial guesses, and four shots to find the solution, the whole procedure would require 21 shots, or an approximate CPU time of 55 seconds. This sample problem has a relatively short heat pipe, which makes accuracy requirements modest; a numerical integration with only 106 steps, requiring 1.4 CPU seconds, gives correct results also. Conversely, for a long heat pipe, higher accuracy is needed, and computation effort increases correspondingly.

VAPOR PRESSURE LOWERING

In a liquid-vapor system at equilibrium in a porous medium, the vapor pressure depends on the geometry of the vapor/liquid interface, the surface tension between these two phases, and on effects of vapor adsorption on the solid grains. Vapor pressure lowering describes the decrease in vapor pressure that occurs when liquid water occupies the small pore spaces in a geologic medium.

Under two-phase conditions, the primary thermodynamic variables are gas-phase pressure P_g , gas saturation S_g , and air partial pressure P_a . When vapor pressure lowering effects are ignored, temperature is determined iteratively from the steam table saturation curve $P_v = P_{sat}(T)$. Since $P_v = P_g - P_a$, the functional dependence of temperature on the primary variables is $T = T(P_g, P_a)$. Vapor pressure lowering can be modeled using the Kelvin equation, in which the capillary pressure function $P_c(S_l)$ accounts for surface tension and interface shape effects. The temperature then depends on saturation as well as vapor pressure, and is given implicitly by

$$P_v = P_{sat}(T) \cdot \exp \left[\frac{P_c(S_l)}{\rho_l R (T + 273.15)} \right] \quad (7)$$

Thus the functional dependence of temperature on the primary variables is $T = T(P_g, P_a, S_g)$. Vapor pressure lowering can have a large effect; when $S_l \rightarrow 1$, $P_c \rightarrow 0$ and $P_v \rightarrow P_{sat}$, but when $S_l \rightarrow 0$,

P_v can decline to a few percent of P_{sat} [11].

Figure 6 shows results for two problems which are identical except for the presence or absence of vapor pressure lowering. The primary differences from the problem described in Table 1 are a factor of order 10^4 decrease in intrinsic permeability and a factor of order 10^2 increase in capillary pressure strength P_{cp} , making this problem more representative of the intact rock at Yucca Mountain. The weaker capillary pressure of the Table 1 problem makes vapor pressure lowering effects negligible in that case. For the problems shown in Figure 6, the intrinsic permeability is too small to allow enough fluid flow for a strong heat pipe to develop (Figure 6b), thus heat transfer is primarily conductive, resulting in linear temperature profiles (Figure 6a). Furthermore, the convective gas-phase flow away from the heat source is small compared to the diffusive mass flow between the air and vapor components of the gas phase, resulting in a non-zero air mass fraction X_g^a in the region near the heat source ($-11 < z < -10$ in Figure 6a). If fracture effects were included, a much stronger heat pipe could develop, depending on various assumptions made about fluid flow in the fractures [3].

The capillary pressure function, slightly modified from the van Genuchten [12] formulation [3] has the feature that P_c becomes very large and negative as $S_l \rightarrow S_{lr}$ (see Table 1). Then, from Equation (7), vapor pressure lowering effects become very strong for small S_l , and the two-phase region extends all the way to z_L , as is shown in Figure 6a. Except for the extension of the two-phase zone to small values of z , inclusion of vapor pressure lowering has only minor impact. The slope of the conductive temperature profile for $-11 < z < -10$ decreases slightly for the vapor-pressure-lowering case (Figure 6a), reflecting the increase in thermal conductivity κ with liquid saturation ($\kappa \sim \sqrt{S_l}$). Variations in fluid flow rate are less abrupt when vapor pressure lowering is included than when it is not (Figure 6b).

SUMMARY AND CONCLUSIONS

The mass and energy transport equations for two-phase fluid and heat flow in one-dimensional radial geometry in a

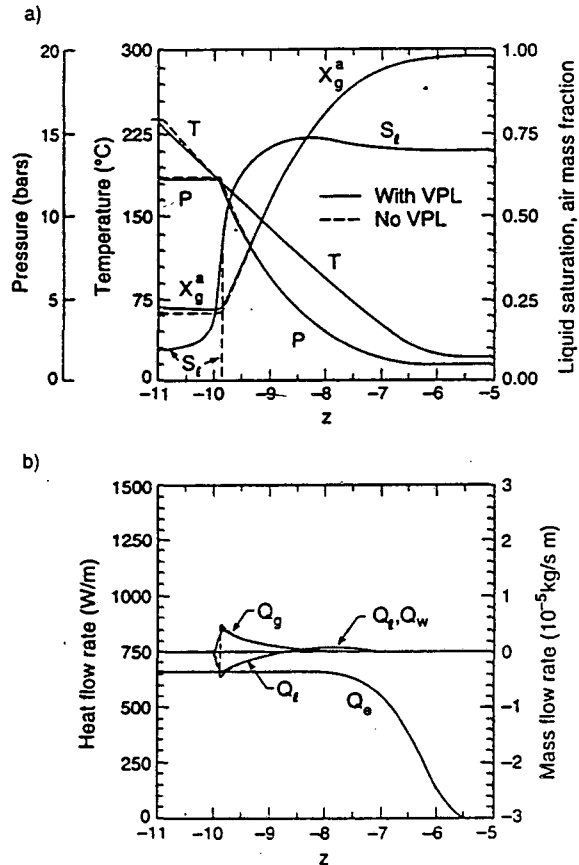


Figure 6. Results of the similarity solution for problems with and without vapor pressure lowering. Note the change of scale for mass flow rate compared to Figure 3.

homogeneous permeable medium depend on time t and distance r only through the similarity variable $\eta = r/\sqrt{t}$. If initial and boundary conditions can be written as functions of η , then the problem is reduced from a set of partial differential equations to a set of ordinary differential equations. A practically important case for which this is possible is a constant-rate line source at $r = 0$ and uniform initial conditions. These boundary conditions give rise to a two-point boundary value problem which can be solved with an iterative integration scheme. We have applied the similarity variable concept to a problem with a linear heat source emplaced in a partially saturated permeable medium, and have discussed the effect of various

parameters in the context of the potential nuclear waste repository at Yucca Mountain, Nevada, although the solution is certainly not limited to this particular application. The similarity solution has been successfully verified by comparison with numerical finite-difference calculations.

One of the strengths of the similarity variable approach is the ability to study the effect of various transport parameters individually, in a simple geometry. Through this exercise one develops a knowledge of basic physical processes, which will be valuable when doing more complicated numerical calculations with realistic geometric detail. The examples in the present paper have illustrated that the presence of air shortens the convective heat-pipe region, thus increasing the temperature at the heat source, and that vapor pressure lowering extends the two-phase region toward the heat source, and makes the onset of counter-flow gradual rather than abrupt.

The similarity-solution results presented here were all calculated using the computer program SIMSOL, which has been fully documented in a laboratory report [13]. In addition to the features described in the present work, the similarity solution can treat an effective continuum representation of a fractured/porous medium, and can include the Klinkenberg approximate treatment of Knudsen diffusion. A detailed description of the similarity solution methodology and results is given in Doughty and Pruess [3,6]. Plans for future work include allowing the inner boundary condition to represent either a heat source or sink, and/or a mass source or sink. This will greatly enhance the applicability of the similarity solution to practical problems, and require only minimal changes to the code. An interesting possible enhancement would be the inclusion of yet another mass component. Components with practical applications include non-condensable gases, (e.g., CO₂), conservative tracers, volatile organic solvents (such as TCE), or non-aqueous phase liquids (hydrocarbon compounds).

ACKNOWLEDGEMENT

The careful review of this work by R. Falta and M. O'Sullivan is greatly appre-

ciated. This work was carried out under U.S. Department of Energy Contract No. DE-AC03-76SF00098, through the Yucca Mountain Project, Sandia National Laboratories, under Document No. SNL 54-1064; numerical computations were supported by the Director, Office of Energy Research, Office of Basic Energy Sciences, Engineering and Geosciences Division, U.S. Department of Energy.

NOTATION

| | |
|-------------|---|
| c | specific heat (J/kg K) |
| D | binary diffusion coefficients (m ² /s) ($D = \tau \phi S_g D_{v_2}^0 P_0/P$) |
| $D_{v_2}^0$ | binary diffusion strength in free gas at $P_0 = 1$ bar (m ² /s) |
| K | mobility (kg/s mPa) ($K_j = k k_{rj} \rho_j / \mu_j$, $j = l, g$) |
| k | intrinsic permeability (m ²) |
| k_r | relative permeability |
| P | pressure (Pa) |
| P_c | capillary pressure (Pa) ($P_c = P_l - P_g$) |
| Q_c | heat flow rate (W/m) |
| Q_w, Q_a | mass flow rates (kg/s m) ($Q_m = Q_l^m + Q_g^m$, $m = w, a$) |
| r | radial distance (m) |
| S | saturation |
| S_{lr} | residual liquid saturation |
| T | temperature (°C) |
| t | time (s) |
| X | mass fraction ($X_l^j + X_g^j = 1$, $j = l, g$) |
| z | integration variable ($z = \ln(\eta) = \ln(r/\sqrt{t})$) |
| η | similarity variable ($\eta = r/\sqrt{t}$) |
| κ | thermal conductivity (W/m K) |
| λ | parameter in van Genuchten characteristic curves |
| μ | dynamic viscosity (Pa s) |
| ρ | density (kg/m ³) |
| ϕ | porosity |
| τ | tortuosity |

Subscripts

| | |
|-----|----------------------------------|
| a | air (also used as a superscript) |
| c | capillary |
| e | energy |
| g | gas phase |
| L | lower limit of integration |

l liquid phase
r relative
sat at saturation (vapor-liquid equilibrium)
s solid
U upper limit of integration
v vapor
w water (also used as a superscript)
0 boundary condition, reference value

LITERATURE CITED

1. Grant, M. A., "Quasi-analytic solutions for two-phase flow near a discharging well," Report 86, Applied Mathematics Division, Dept. of Scientific and Industrial Research, Wellington, New Zealand (1979).
2. O'Sullivan, M., J., Water Resour. Res. 17(2), 390-398 (1981).
3. Doughty, Christine and Karsten Pruess, "A similarity solution for two-phase water, air, and heat flow near a linear heat source in a porous medium," Report LBL-30051, Lawrence Berkeley Lab., Berkeley, CA (1991).
4. International Formulation Committee, A formulation of the thermodynamic properties of ordinary water substance, IFC Secretariat, Duesseldorf, Germany (1967).
5. Press, W. H., B. P. Flannery, S. A. Teukolsky, and W. T. Vetterling, Numerical recipes: the art of scientific computing, Cambridge University Press, New Rochelle, New York, Ch. 16 (1986).
6. Doughty, Christine and Karsten Pruess, Int. J. Heat Mass Transfer 33(6), 1205-1222 (1990).
7. Pruess, Karsten, Y. W. Tsang, and J. S. Y. Wang, Water Resour. Res. 26(6), 1235-1248 (1990).
8. Pruess, Karsten, "TOUGH user's guide," Report NUREG/CR-4645, Nuclear Regulatory Commission, Washington, D.C. (1987). (Also avail. as Lawrence Berkeley Lab. Report LBL-20700.)
9. Pruess, Karsten, "TOUGH2-A general-purpose numerical simulator for multiphase fluid and heat flow," Report LBL-29400, Lawrence Berkeley Lab., Berkeley, CA (1990).
10. Narasimhan, T. N. and P. A. Witherspoon, Water Resour. Res. 12(1), 57-64 (1976).
11. Hsieh, C. H. and H. J. Ramey, Jr., Soc. Pet. Eng. J. 23, 157-167 (1983).
12. van Genuchten, M. Th., Soil Sci. Soc. Am. J. 44, 892-898 (1980).
13. Doughty, Christine, "SIMSOL Users Guide," Report LBL-28384, Lawrence Berkeley Lab., Berkeley, CA (1991).

LAWRENCE BERKELEY LABORATORY
UNIVERSITY OF CALIFORNIA
INFORMATION RESOURCES DEPARTMENT
BERKELEY, CALIFORNIA 94720